JCI insight

BTK inhibitor-induced defects in human neutrophil effector activity against *Aspergillus fumigatus* are restored by TNFα

Diego A. Vargas-Blanco, … , Jeremy S. Abramson, Jatin M. Vyas

JCI Insight. 2024. https://doi.org/10.1172/jci.insight.176162.

Research In-Press Preview Immunology Infectious disease

Graphical abstract

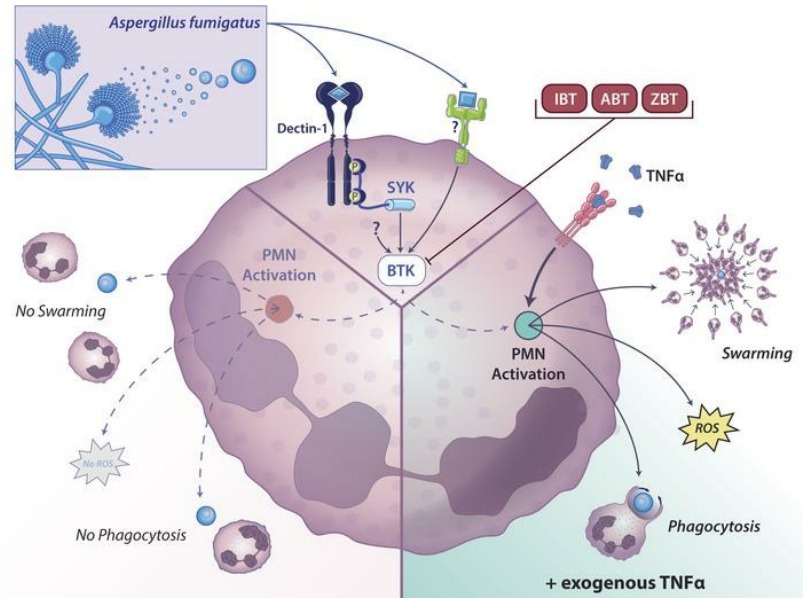

BTK inhibitor-induced defects in human neutrophil effector activity against *Aspergillus fumigatus* are restored by TNFα

Diego A. Vargas-Blanco[1, 2,*], Olivia W. Hepworth[1, 2,*], Kyle J. Basham[1], Patricia Simaku[1], Arianne J. Crossen[1], Kyle D. Timmer[1], Alex Hopke[2-4,%], Hannah Brown Harding[1,2], Steven R. Vandal[5], Kirstine N Jensen[1,2], Daniel J. Floyd[1], Jennifer L. Reedy[1,2], Christopher Reardon[1], Michael K. Mansour[1, 2], Rebecca A. Ward[1], Daniel Irimia[2-4], Jeremy S. Abramson[6], and Jatin M. Vyas[1, 2, #]

[1]Division of Infectious Diseases, Department of Medicine, Massachusetts General Hospital, Boston, MA; [2]Harvard Medical School, Boston, MA; [3]BioMEMS Resource Center, Massachusetts General Hospital, Boston, MA; [4]Shriners Hospital for Children, Boston, MA; [5]Beth Israel Deaconess Medical Center, Boston, MA; [6]Center for Lymphoma, Mass General Cancer Center, Boston, MA; [*]co-first authors; [%]current institution: Department of Biomedical Sciences, Quillen College of Medicine, Center for Inflammation, Infectious Disease and Immunity, East Tennessee State University, Johnson City, TN

Correspondence: Jatin M. Vyas, Massachusetts General Hospital, 55 Fruit Street, Boston, MA 02114, US; jvyas@mgh.harvard.edu.

ABSTRACT

Inhibition of Bruton's tyrosine kinase (BTK) through covalent modifications of its active site (*e.g.,* ibrutinib [IBT]) is a preferred treatment for multiple B cell malignancies. However, IBT-treated patients are more susceptible to invasive fungal infections, although the mechanism is poorly understood. Neutrophils are the primary line of defense against these infections; therefore, we examined the impact of IBT on primary human neutrophil effector activity against *Aspergillus fumigatus*. IBT significantly impaired the ability of neutrophils to kill *A. fumigatus* and potently inhibited reactive oxygen species (ROS) production, chemotaxis, and phagocytosis. Importantly, exogenous TNFα fully compensated for defects imposed by IBT and newer-generation BTK inhibitors and restored the ability of neutrophils to contain *A. fumigatus* hyphal growth. Blocking TNFα did not impact ROS production in healthy neutrophils but prevented exogenous TNFα from rescuing the phenotype of IBT-treated neutrophils. The restorative capacity of TNFα was independent of transcription. Moreover, the addition of TNFα immediately rescued ROS production in IBT-treated neutrophils indicating that TNFα worked through a BTK-independent signaling pathway. Finally, TNFα restored effector activity of primary neutrophils from patients on IBT therapy. Altogether, our data indicate that TNFα rescues the antifungal immunity block imposed by inhibition of BTK in primary human neutrophils.

INTRODUCTION

Invasive fungal infections are dreaded complications for those with compromised immune systems, including cancer patients (*e.g.,* leukemia, lymphoma), solid-organ and hematopoietic stem cell transplant recipients. The fungal pathogen *Aspergillus* spp. causes a spectrum of diseases, including asthma, chronic infection, and invasive disease. Invasive fungal infections carry elevated mortality rates in these high-risk patients, despite the availability of antifungals(1-4), demonstrating the critical role of the innate immune system as the first line of defense against these devastating infections (5, 6).

As the first responders in fungal infections, neutrophils exert antifungal activity through multiple effector functions, including swarming, phagocytosis, and reactive oxygen species (ROS) production. Activation of neutrophil pattern recognition receptors triggers these effector functions and subsequent cytokine secretion. However, a reduced ability to produce neutrophils or neutrophil dysfunction occurs in many immunosuppressed individuals, contributing to an elevated risk of invasive fungal infections, including invasive aspergillosis. Tyrosine kinases are critical to neutrophil effector function in antifungal immunity (7-9). *Aspergillus* cell wall carbohydrates trigger intracellular signaling cascades and effector functions through spleen tyrosine kinase (Syk) (10, 11). Bruton's tyrosine kinase (BTK), a kinase downstream of Syk, mediates antifungal response in innate immune cells, including neutrophils (12). While these kinases are critical in antifungal immunity, small-molecule inhibitors targeting these molecules are effective therapeutics for B cell malignancies and chronic graft-versus-host disease (13-16).

Unfortunately, BTK inhibitor therapy amplifies the risk of invasive infections, including fungal pathogens, particularly in dissemination to the central nervous system (CNS) (15, 17-20). Although BTK inhibitors (*e.g.,* acalabrutinib [ABT], ibrutinib [IBT], zanubrutinib [ZBT]) improve

outcomes in multiple subtypes of B cell lymphoma and leukemia, BTK and other Tec protein tyrosine kinases signal diverse cellular processes in immune cell lineages (*e.g.,* macrophages, neutrophils, γδ T cells) (21-24). These BTK inhibitors impair the function of immune cells critical to host defense against invading pathogens through the suppression of pro-inflammatory cytokines, dampened killing capacity, and blunted ROS production (19, 25-32). Indeed, the irreversible inhibitor of BTK, IBT, quickly reduces BTK phosphorylation at the Tyr^{551} and Tyr^{223} sites and has been linked to defects in murine neutrophils when responding to *A. fumigatus* (29, 31). The impact of BTK inhibition on neutrophil effector functions remains incompletely understood (33).

Here, we demonstrate the deleterious effect of three BTK inhibitors (IBT, ABT, and ZBT) on the antifungal effector functions of human neutrophils including chemotaxis, phagocytosis, and ROS production. Given that genes related to the TNF signaling pathways were the most differentially expressed in IBT-treated neutrophils, we tested the hypothesis that TNFα could bypass the block imposed by BTK inhibition. We show that exogenous TNFα improves BTK inhibitor-associated defects, restoring the neutrophil ability to control *A. fumigatus* in healthy neutrophils treated with BTK inhibitors as well as in neutrophils from IBT-treated patients. We demonstrate that the restorative effect of exogenous TNFα occurs via transcription-independent signaling. Taken together, these data indicate that exogenous TNFα acts as a signaling molecule in neutrophils, rapidly compensating for BTK inhibitor-imposed defects in response to *A. fumigatus*.

RESULTS

Ibrutinib inhibited neutrophil effector activity against *A. fumigatus*

To evaluate the hypothesis that BTK inhibition of neutrophils affect antifungal immune response against *A. fumigatus*, we sought to determine the impact of BTK inhibition on neutrophil effector functions including killing, ROS production, phagocytosis, and swarming by neutrophils when challenged with *A. fumigatus*. Primary human neutrophils treated *ex vivo* with IBT at a physiologically relevant concentration (19, 34) (0.3 μM) or ten-fold higher or lower concentrations failed to kill *A. fumigatus* in contrast to neutrophils treated with solvent control (0.1% DMSO), as shown by a resazurin-based metabolic assay (***Figure 1A***). These data were confirmed by calculating the rate of growth inhibition of *A. fumigatus* when compared to the *A. fumigatus* growth alone (***Figure 1B***). These results demonstrated that IBT-treated neutrophils failed to control *A. fumigatus* growth as compared to solvent-treated neutrophils.

We next examined the effects on ROS production in primary neutrophils using the same doses as above. Consistent with the metabolic activity assay, IBT-treated neutrophils produced less ROS in response to heat-killed *A. fumigatus* hyphae when compared to DMSO-treated neutrophils (***Figure 1C***). These BTK inhibitor-induced effects on ROS production were not strain-specific and IBT blocked β-glucan-coated bead (the agonist for Dectin-1 signaling) induced ROS production (***Supplemental Figure 1A-D***). As a control, we examined the impact of BTK inhibition on Dectin-1 expression in primary human neutrophils as loss of expression of Dectin-1 could be a trivial explanation for these findings. Dectin-1 expression was not altered in IBT-treated neutrophils (***Supplemental Figure 1E***). To examine whether these effects blocked all induced ROS production, we stimulated IBT-treated neutrophils with PMA, a NADPH oxidase inducer. PMA in the presence of IBT generated ROS similar to the solvent control (***Figure 1D***), suggesting

that IBT-associated ROS defects were specific to ligands found on *A. fumigatus*. We examined intracellular ROS production to determine if this process was also sensitive to BTK inhibition. IBT potently reduced the amount of intracellular ROS as determined by flow cytometry (***Supplemental Figure 2***). These data indicate that IBT blocked both extracellular and intracellular ROS production.

Since pathogen-associated molecular pattern molecules can trigger an increase of neutrophilic phagocytic activity (35), we sought to determine if BTK inhibitor effect included phagocytosis. We measured neutrophil phagocytosis of *A. fumigatus* by flow cytometry using AF488-labeled conidia. Neutrophils were gated as the double positive $CD45^+/CD66b^+$ subpopulation and evidence of phagocytosis was defined as $CD45^+/CD66b^+/Af488^+$. Neutrophil phagocytosis of *A. fumigatus* conidia was severely impaired by IBT in a dose-dependent manner when compared to solvent-treated neutrophils (***Figure 1E, panel 1-3***). To rule out stochastic associations of conidia and neutrophils at a superficial level, we used cytochalasin D, an actin polymerization inhibitor, in parallel treatments for each condition tested. In the presence of cytochalasin D, $CD45^+/CD66b^+/AF488^+$ events were below 1.35% for solvent-treated neutrophils (***Figure 1E, panel 4***), with similar values for all other neutrophil treatments (***Supplemental Figure 3***). These results indicated that IBT-treated human neutrophils were impaired in their phagocytic capacity as compared to solvent-treated neutrophils.

We next leveraged a neutrophil swarming assay (36) to determine how coordinated chemotaxis to the site of infection and containment of fungal growth may be impacted by BTK inhibition. We observed significantly impaired neutrophil swarming over 200 min towards *A. fumigatus* in IBT-treated neutrophils compared to the solvent control (***Figure 1F-G***). In addition,

we demonstrated that IBT-treated neutrophils were less able to contain fungal growth compared to solvent-treated neutrophils 16h after co-incubation of *A. fumigatus* (***Figure 1H***).

TNFα compensated IBT-induced defects in neutrophils against *A. fumigatus*

To better understand how BTK impacted the neutrophil immune response against *A. fumigatus,* we assessed signaling pathways affected by IBT treatments at the transcript level. We collected RNA from unstimulated neutrophils treated with either 0.3 μM IBT or solvent control for 4h and assessed the expression of 773 host response genes. Using NanoString nCounter, we detected 18 differentially expressed genes (DEGs) in IBT- vs solvent-treated unstimulated neutrophils (***Figure 2A, Table 1, Supplemental Table 1***). Interestingly, *TNF* was the top hit and was downregulated by a $\log_2$ fold-change of 4, closely followed by *CD274* whose product PD-L1 has been positively correlated with TNFα production (37, 38). Moreover, *RAC2*, important for neutrophil granule exocytosis (39) and TNFα-mediated ROS production (40) was found to be upregulated. Given the role of multiple DEGs in TNFα signaling pathways, we next examined upregulated and downregulated genes in the TNFα pathway using a KEGG map (***Figure 2B***). The analysis revealed that the genes *ADGRG3, ALPL, CR1, ERN1, FOS, IL1RAP, IL1RL1, MAP2K4, PIK3CB, RAC2, TIMP2,* and *TME140* were upregulated or relatively unchanged. Downregulation of *APOL6, CD274, FBXO6, GBP1, STAT1,* and *TNF* occurred in IBT-treated neutrophils.

Analysis of transcriptional changes in IBT-treated neutrophils revealed that the TNF signaling pathway was the most affected. We hypothesized that exogenous TNFα could rescue the immune defects in these neutrophils. Most TNFα in inflammatory conditions are from heterologous sources (*e.g.,* macrophages, dendritic cells), with a small fraction made from neutrophils. To address their contribution, we quantified soluble TNFα by ELISA using the

supernatant of *A. fumigatus*-stimulated neutrophils. Indeed, TNFα levels were 45% lower in IBT-treated cells compared to the solvent control (***Supplemental Figure 4A***). To test the hypothesis that exogenous TNFα can restore neutrophil activity against *A. fumigatus*, we stimulated IBT-treated neutrophils with recombinant TNFα, then challenged with *A. fumigatus*. At both 5 ng/mL and 100 ng/mL, TNFα restored effector activity against *A. fumigatus* to levels comparable to those of competent neutrophils, as demonstrated by growth inhibition (***Figure 3A***) and ROS production (***Figure 3B, Supplemental Figure 4-5***). Similarly, TNFα promoted neutrophil swarming in IBT-treated neutrophils recapitulating those of control neutrophil treatments (***Figure 3C-E***). TNFα also restored the phagocytic activity of 0.3 μM IBT-treated neutrophils (2.36% phagocytic activity, ***Figure 1E***) compared to 63.6% and 68.2% when 5 ng/mL or 100 ng/mL TNFα were added, respectively (***Figure 3F, Supplemental Figure 5C***). We then examined the transcription signature of IBT-treated neutrophils stimulated with *A. fumigatus* with and without exogenous TNFα. Out of 773 genes examined by NanoString nCounter, 79 were DEG in IBT-treated vs solvent control-treated neutrophils stimulated with *A. fumigatus*, 65 of which were compensated (genes not significantly dysregulated for IBT+TNFα vs solvent control) by 5 ng/mL TNFα (***Figure 3G, Supplemental Table 1***). Taken together, our data indicated that TNFα, at doses as low as 5 ng/mL, compensated for IBT-induced defects in neutrophils.

In addition to TNFα, we tested the effect of IFNγ, G-CSF, IL-1β, and IL-8, on neutrophils treated with 0.3 μM and 3 μM IBT. The effects of GM-CSF on neutrophil function following BTK inhibition is discussed in Desai et al (41). However, IFNγ, G-CSF, IL-1β, and IL-8 did not restore neutrophil effector activity but rather further exacerbated the IBT-associated defects for killing capacity against *A. fumigatus* (***Supplemental Figure 6A***). Importantly, growing *A. fumigatus* in presence of IBT or any of these cytokines alone did not alter the pathogen's basal metabolic

activity (*data not shown*). While the killing capacity was not compensated by these cytokines, G-CSF mildly improved extracellular ROS production. Similarly, IFNγ, IL-1β, and IL-8 showed a modest increase (***Supplemental Figure 6B***). Neither TNFα nor all other tested cytokines elicited neutrophil ROS production in the absence of a stimulant. Additionally, neutrophil swarming and phagocytosis defects were not improved by exogenous IFNγ, G-CSF, IL-1β, and IL-8 in IBT-treated neutrophils (***Supplemental Figure 6C-E***). These data indicated that TNFα, specifically, restored the defects caused by BTK inhibition on human neutrophil effector activity.

TNFα improved effector function defects imposed by other BTK inhibitors

Patients treated with IBT carry an increased risk for invasive fungal infections (15). However, patients on newer agents in this class rarely report significant invasive fungal infections (42-46). It remains unclear whether these agents behave differently with respect to *A. fumigatus*-specific neutrophil effect activity. To determine if other FDA-approved BTK inhibitors affected antifungal immunity, we used ABT and ZBT, newer generation BTK inhibitors with reported decreased off-target activity (47, 48). Using the growth inhibition measurement, both drugs at physiologically relevant concentrations (1 μM for ATB and 0.4 μM for ZBT) (49-52) or ten-fold below disrupted immunological mechanisms implicated in *Aspergillus* defense (***Figure 4A***), confirming that BTK inhibition dampened the neutrophil response against *A. fumigatus*. Therefore, we considered whether TNFα could compensate the specific defects imposed by ABT and ZBT in neutrophils. We measured *A. fumigatus* killing, ROS production, phagocytosis, and swarming in ABT- and ZBT-treated neutrophils. These experiments revealed similar outcomes to those elicited by IBT, all of which TNFα rescued to similar levels as the solvent controls (***Figure 4A-G; Supplemental***

194 ***Figure 7***). Taken together, our observations indicated a class-effect of BTK inhibitors that is not
195 limited to a specific drug in this family of chemotherapeutic agents.
196
197 **Restorative capacity of exogenous TNFα was transcription-independent**
198 Since IBT treatment impaired TNFα production in neutrophils stimulated with *A. fumigatus*, we
199 sought to determine whether endogenously produced TNFα contributed to the ability of
200 neutrophils to respond to *A. fumigatus*. We treated neutrophils with infliximab (IFM), a
201 monoclonal antibody to TNFα, prior to stimulation with *A. fumigatus* and demonstrated no changes
202 in pathogen killing or ROS production compared to the solvent control (***Figure 5A-B***). Moreover,
203 adding IFM to IBT-treated neutrophils prior to the addition of TNFα showed no change in
204 pathogen killing efficiency. However, there was modest ROS production, probably caused by
205 partial activation of the TNFα receptor.
206 To assess whether the rescue of neutrophil effector activity by TNFα required *de novo*
207 transcriptional activity, we assessed if exogenous TNFα utilizes pre-existing signaling pathways.
208 We treated neutrophils with IBT or solvent control for 30 min, followed by TNFα immediately
209 before stimulation with *A. fumigatus* (0 min), 15 min, or 30 min. TNFα rescued ROS production
210 even when the cytokine was added immediately before stimulation, with the starting signal
211 detected 20 min after stimulation (***Figure 5C***), demonstrating a swift response prior to expected
212 transcriptional changes. To address directly the role of transcription in this process, neutrophils
213 treated with IBT for 30 min were exposed to actinomycin D (actD), a potent transcription inhibitor
214 (53), for 15 min and supplemented with TNFα. Compensation of ROS production by TNFα
215 occurred even in the absence of transcription (***Figure 5D***). These data indicated that TNFα acted

through BTK-independent signaling pathway(s) to promote ROS production, without the need for transcription.

Exogenous TNFα rescued defects in neutrophils from patients undergoing treatment with IBT

Our data demonstrated that treating primary healthy human neutrophils with BTK inhibitors *ex vivo* potently affected neutrophil effector activity against *A. fumigatus*, a defect that exogenous TNFα restored. However, whether this observation translated to patients on BTK inhibitors for the management of oncologic diagnosis remained unclear. Thus, we examined the restorative effect of TNFα on the neutrophil immune response against *A. fumigatus* in patients actively treated with IBT. We isolated neutrophils from B-lymphocyte leukemia patients undergoing IBT therapy. Patient or healthy donor neutrophils were treated with TNFα for 3h, followed by stimulation with *A. fumigatus*. We then quantified pathogen killing, ROS production, and phagocytosis. Our results recapitulated our previous data: neutrophils from IBT-treated patients were less effective at responding to *A. fumigatus* when compared to neutrophils from healthy donors, but TNFα rescued these defects to healthy control baseline (***Figure 6, Supplemental Figure 8***). Together, these data demonstrated that BTK inhibitor-mediated neutrophil dysfunction can be reversed by TNFα from patients on chronic IBT therapy.

DISCUSSION

Here, we unveiled the role of BTK inhibition on neutrophil antifungal effector functions. Specifically, we demonstrated that even below typical plasma concentrations seen in chronically treated patients, BTK inhibitors caused significant immune defects in human neutrophils against the fungal pathogen. We identified TNFα as one of the major pathways modified at a transcriptional level by BTK inhibition in neutrophils. Furthermore, we showed that exogenous TNFα restores critical effector functions to contain and neutralize *A. fumigatus.* Importantly, these effects were not exclusive to healthy human neutrophils, but also observed in neutrophils isolated from B-lymphocyte leukemia patients receiving IBT treatment. Together, these data suggest that BTK functions as a master regulator of antifungal neutrophil activity.

Recognition of fungal cell wall components such as β-glucan and galactomannan by immune cells triggers antifungal immunity through phagocytosis, chemotaxis, production and release of pro-inflammatory cytokines, and ROS production (5). These pathways rely on the activation of tyrosine kinases, including BTK, to mediate immune effector functions to invading pathogens. Indeed, carbohydrate-like receptors (CLRs), integrins, Toll-like receptors (TLRs), and the inflammasome are the primary activators of antifungal signaling cascades (54, 55). The integrin receptor CD11b/CD18 (Mac-1) and the CLR Dectin-1 are important receptors for β-glucan recognition in humans (56, 57), and participate in granulocyte activation, chemotaxis, cytotoxicity, and phagocytosis (58-61). We show that BTK does not abrogate Dectin-1 expression on IBT-treated neutrophils. The recognition of fungal hyphae or large clusters of conidia, potentially mediated by the same receptors, triggers neutrophil cooperation observed during swarming (39). Importantly, Mac-1 and Dectin-1 signals through kinases such as Syk, PI3K, and PKC (62), which in turn can modulates BTK activity. Interestingly, Mac-1 activation requires BTK in sterile

inflammation (63). Activation of these pathways mediates the production of pro-inflammatory cytokines, phagocytosis of pathogens, and confinement of growing fungi inside neutrophil swarms (7). Although critical for antifungal immunity, these responses vary between immune cell types. In murine macrophages stimulated with *A. fumigatus*, TLR9-BTK-calcineurin-NFAT signaling cascade requires Dectin-1 and Syk-dependent phagocytosis, yet no changes in phagocytosis occur in response to inhibition of BTK (25, 64). Interestingly, in response to the fungal organism *Candida albicans* in macrophages, BTK localizes to the phagocytic cup and is necessary to generate mature phagosomal markers (9). Furthermore, BTK inhibition dampens phagocytic uptake. In the present study, we revealed the importance of functional BTK in mediating phagocytic uptake of *Aspergillus* conidia. While prior studies in macrophages suggest that phagocytosis of *A. fumigatus* remains similar in the presence and absence of BTK inhibition (63), it is possible that immortalized cell lines and primary human neutrophils respond differently. These data suggests that that role of BTK in phagocytosis may be species- and immune-cell specific. The precise mechanism of BTK modulation of phagocytosis in neutrophils remains unknown.

Neutrophil ROS production facilitates fungal killing. Inadequate production of ROS enables fungal pathogens to invade host tissues. Individuals with deficiencies in key components of ROS production, such as subunits of the NADPH oxidase complex, are at risk of recurrent and severe fungal infections (65, 66), highlighting the importance of ROS in containing fungal infections. Given the reduced phagocytic capacity of neutrophils treated with BTK inhibitors, we would expect reduced downstream ROS production. Indeed, our data suggest that BTK inhibition only impairs phagocytosis-dependent intracellular and extracellular ROS production in response to *A. fumigatus*. These data confirm previous studies that demonstrate dampened ROS production in neutrophils isolated from patients with one month and three months of IBT therapy (18). Since

most of our investigations utilized neutrophils isolated from healthy volunteers, these results suggest that the reduction of effector functions against *A. fumigatus* is triggered by the BTK inhibition rather than the underlying disease requiring treatment with BTK inhibitors (*e.g.,* chronic lymphocytic leukemia, graft-versus-host disease). Overall, we argue that BTK regulates neutrophil phagocytosis, a fundamental step in the recognition of fungal pathogens, which subsequently leads to ROS production and ultimately the killing of the pathogen.

Cases of aspergillosis dominate the invasive fungal infections in patients receiving BTK inhibitory therapy compared to other fungal pathogens. Interestingly, there is a proclivity of disseminated *Aspergillus* infection to the CNS in patients treated with a BTK inhibitor, with 40-60% of IBT-associated aspergillosis presenting cerebrally (20, 43, 67, 68). The mechanisms underpinning the susceptibility of the CNS to invasive aspergillosis remains unknown. While the role of BTK inhibition in innate immune cells in the periphery has been demonstrated by data presented here and in other studies, the role of BTK inhibition on resident immune cells (*i.e.,* microglia and astrocytes) in the brain or the blood-brain barrier function in the setting of fungal infection remains unknown. BTK inhibition dampens microglial and astrocyte lipopolysaccharide-induced activation and proinflammatory cytokine production, including TNFα (69). Here, we suggest that neutrophil dysfunction is important to BTK inhibition-associated aspergillosis. In a model of cerebral aspergillosis, no change in the number of neutrophil or γδ T cells were observed, although other immune cells were drastically lower (70). Neutrophils produce low levels of TNFα compared to other inflammatory cells, such as macrophages, dendritic cells, natural killer cells, and T cells (71). Perhaps these cells compensate for the decreased TNFα produced by neutrophils during treatment with BTK inhibitors, resulting in less established fungal infections in the periphery. Given the immunomodulatory role of IBT in a murine model and the fact that microglia,

304 astrocytes, and neurons are the primary source of TNFα in the CNS (69, 72), it is possible that low
305 TNFα secretion cannot be compensated in the brain, enabling fungal organisms to establish an
306 infection in patients receiving BTK inhibition. Further investigations on the role of local and
307 recruited immune cells in BTK inhibition-associated CNS aspergillosis are warranted.

308 Given the propensity of invasive fungal infections in patients treated with BTK inhibitors,
309 we examined opportunities to bypass BTK inhibition and restore neutrophil effector functions. Our
310 transcriptional analyses highlight an upregulation of numerous components in the TNFα signaling
311 pathway, including the receptor. Interestingly, we reveal a downregulation of TNFα itself in BTK
312 inhibited neutrophils. In concordance with these observations, BTK inhibition impairs TNFα
313 production in monocyte-derived macrophages, alveolar macrophages, and γδ cells in response to
314 *A. fumigatus, Streptococcus pneumoniae*, and *Mycobacterium tuberculosis* (25, 26, 28, 64). Since
315 TNFα can modulate neutrophil recruitment, an insufficient production of TNFα by macrophages
316 and γδ cells in response to *Aspergillus* may contribute to blunted neutrophil recruitment and host
317 defense in patients treated with BTK inhibitors.

318 Since TNFα was downregulated, we hypothesized that exogenous TNFα could restore
319 neutrophil effector function, despite other pathway components remaining available. Upon
320 exposure to exogenous TNFα, BTK-treated neutrophils recovered effector activity. While these
321 results are encouraging, the use of TNFα during fungal infections in patients treated with a BTK
322 inhibitor is not feasible given the numerous off-target effects and induction of severe endotoxic
323 shock. TNFα is an essential proinflammatory cytokine, but under certain circumstances, too much
324 TNFα indirectly induces cell death through amplified proinflammatory response (73). Due to
325 exacerbated inflammation, anti-TNFα biologics are approved for autoimmune diseases such as
326 rheumatoid arthritis, psoriasis, Crohn's disease, and ulcerative colitis (74). These TNF antibody

treatments carry an increased risk of fungal infection, particularly in those treated for gastrointestinal disease (75, 76). Thus, understanding how exogenous TNFα exerts protective effects may expand beyond BTK inhibitor treatments to include high-risk patients on TNF biologics. Further studies are warranted to identify downstream targets with better therapeutic potential in these patients.

Here, we reveal that stimulation of the TNFα signaling pathway compensates for defects in neutrophils chronically exposed to IBT. GM-CSF can also compensate for these defects (41), while IFN-γ. G-CSF, IL-1β, and IL-8 were unable to do so. Notably, both GM-CSF and TNFα converge on the PI3K/AKT pathway, which may provide insight into the specificity of this response. A small molecule that activates this pathway may be another approach to overcome the effects of BTK inhibition. Thus, further research will seek to understand better the specific effectors downstream of TNFα supplementation responsible for the rescue of neutrophil defects induced by BTK inhibitor treatments to enable more targeted therapies. Overall, the results presented here significantly enhance our insights into the immunomodulatory properties of BTK inhibition and identify pathways that may be leveraged to improve patient outcomes.

METHODS

Sex as a Biological Variable

Neutrophils were isolated from both men and women. No differences in were observed between these groups. All data shown in this manuscript represent pooled samples from neutrophils isolated from both men and women in the given treatment group.

Strains and culture conditions

A. fumigatus strains B5233 (77), Af293 (78), ATCC46645 (79), and CEA10 (80, 81) were grown in glucose minimum media (GMM) agar at 37°C for three days. Conidia were harvested using sterile water with 0.01% Tween 20 and purified using a 40-μm cell strainer. Spores were washed three times with sterile PBS and counted on a LUNA^{TM} automated cell counter (Logos Biosystems, Annandale, VA). Swollen conidia were obtained by incubating *A. fumigatus* conidia in cRPMI media (RPMI-1640 [Corning, Corning, NY, catalog #10-040-V] supplemented with 9% FBS [Life Technologies, Carlsbad, CA, catalog #26140079], 158 μM penicillin, 152 μM streptomycin, 1.8 mM L-glutamine, 9 mM HEPES, 63.3 μM β-mercaptoethanol) in the presence of 0.5 mg·mL^{-1} voriconazole (VRZ; Sigma-Aldrich, St. Louis, MO, Catalog #PZ0005-25MG) for 6h at 30°C with agitation. Swollen conidia were centrifuged for 3 min at 16,000 x g, washed with sterile PBS three times, and resuspended in cRPMI.

Heat-killed *A. fumigatus* was grown as previously described (82). Briefly, 3x10^7 colony forming units were inoculated in 5 mL of YPD media (yeast extract, peptone, dextrose) and grown at 37°C overnight to generate hyphae. Mycelium was carefully collected, centrifuged for 3 min at 16,000 x *g*, washed with sterile PBS three times, weighted, and resuspended in 1 mL of PBS. Hyphae was heat-killed using three 95°C cycles of 10-min each, vortexing between cycles. Heat-

killed hyphae was grinded using sterile 1.5-mL pestles (Bio Plas, Inc., San Rafael, CA, Catalog #4030-PB). Grounded heat-killed hyphal elements were washed three times in PBS and resuspended to 1 mg of material per mL and stored at 4°C.

Human neutrophil isolation

Peripheral blood from eighteen healthy volunteers and five B-lymphocyte leukemia patients treated with IBT were collected in K2 EDTA-treated tubes (BD, Franklin Lakes, NJ, Catalog #367899) and centrifuged at 1,500 x g for 15 min at room temperature. Neutrophils were isolated from the buffy coat by negative isolation using the EasySep™ Direct Human Neutrophil Isolation Kit (STEMCELL Technologies Inc., Cambridge, MA, Catalog #19666), according to the manufacturer's instructions. Isolated neutrophils were resuspended in cRPMI, assessed viability using Acridine Orange / Propidium Iodide (New England BioGroup, Atkinson, NH, Catalog #F23001), and analyzed by flow cytometry to confirm purity using a BD FACSCelesta Cell Analyzer and the Diva software (BD Biosciences, Billerica, MA). All data shown are representative of at least three independent experiments using different donors.

Drugs, cytokines, and monoclonal antibody treatments

Unless stated otherwise, neutrophils were incubated with ABT, IBT, ZBT (Cayman Chemical, Ann Arbor, MI, Catalog #19899, #16274, and #28924, respectively), or the solvent vehicle control (0.1% DMSO) at the indicated concentrations for 4h at 37°C and 5% CO_2. When necessary, a 4h cytokine treatment started 30 min after adding the BTK inhibitor. The following cytokines and their doses were used: 5 ng/mL and 100 ng/mL TNFα (Invivogen, San Diego, CA, Catalog #rcyc-htnfa); 100 ng/mL IFNγ (BioLegend, San Diego, CA, catalog #570206); 100 ng/mL IL-1β, 50

ng/mL IL-8, or 100 ng/mL G-CSF (PeproTech, Cranbury, NJ #200-01B, #200-08M, #315-02, respectively).

For blocking of phagocytosis, 20 μM of cytochalasin D (Sigma-Aldrich, St. Louis, MO, Catalog #C8273-1MG) was used prior to adding any treatment. For TNFα blocking experiments, 25 μg/mL infliximab (IFM; MGH Pharmacy) was added 15 min before adding TNFα. For the TNFα time-course experiment, neutrophils were treated with 5 ng/mL TNFα for 0-, 15-, or 30-min stimulation with *A. fumigatus*. For transcription inhibition experiments, 1 μg/mL actinomycin D (actD); Sigma-Aldrich, St. Louis, MO Catalog #A1410-2MG) was used 30 min after adding IBT. Cytokines were added 15 min after actD.

Aspergillus metabolic assay (neutrophil killing assay)

Neutrophils were treated with DMSO or either ABT, IBT, or ZBT as described above. Unless stated otherwise, 200,000 neutrophils/well were stimulated with 50,000 *A. fumigatus* swollen conidia in Falcon 96-well plates (Corning, Corning, NY, catalog #353219). VRZ was used at 16 μg/mL as a control for suppression of *A. fumigatus* metabolic activity. After 5h, neutrophils were lysed using NP-40 lysis buffer (75 mM NaCl, 2.5 mM $MgCl_2 \cdot 6H_2O$, 0.5% NP-40, pH 7.5) for 5 min on ice. Media was then supplemented with MOPS-cRPMI (cRPMI containing 165 mM MOPS, 2% glucose, pH 7.0) and 1:10 PrestoBlue (Invitrogen, Waltham, MA catalog #A13261), and conidia were allowed to germinate for 12.5h at 37°C. Thereafter, fluorescence (560/590 nm) was recorded every 30 min for 24h. *A. fumigatus* metabolic activity was determined by resorufin fluorescence using an SpectraMax i3x microplate reader (Molecular Devices, San Jose, CA). *A. fumigatus* killing was estimated using the Gompertz function as described below:

$$Y = Y_M \left(\frac{Y_0}{Y_M}\right)^{e^{-Kt}}$$

Where Y_0 is the starting metabolic activity, Y_M is the maximum metabolic activity, K describes the metabolic rate, or equivalently $1/K$ the delay (inflection point). We estimated *A. fumigatus* killing by finding the ratio of Y_0 of a neutrophil and *A. fumigatus* treatment with respect to the Y_0 of an *A. fumigatus* control condition (*i.e.,* spores only, IBT treatment) as described below.

$$Growth\ inhibition,\ \% = \left(1 - \frac{Y_0,\ treatment}{Y_0,\ control\ condition}\right) \cdot 100\%$$

For all figures, the data are presented as the percent of growth inhibition after performing the linear regression analysis using Gompertz fit with 95% confidence intervals (with the exception of 1A-B, which shows the raw data used to calculate the growth inhibition in A). All raw data are provided in the supplemental data found on the JCI Insight website.

Neutrophil extracellular ROS production

Using 96-well plates (Greiner Bio-One, Monroe, NC, catalog #655083), 100,000 neutrophils in cRPMI were stimulated for 4h at 37°C with 1 mg/mL *A. fumigatus* heat-killed hyphae, 1 μg/mL phorbol 12-myristate 13-acetate (PMA; STEMCELL Technologies Inc., Cambridge, MA, catalog #74042), or β-glucan-coated beads (83) at 5:1 bead-to-neutrophil ratio in presence of 0.15 μM lucigenin (bis-N-methylacridinium nitrate; Enzo Life Sciences Inc., Farmingdale, NY, catalog #ENZ-52154) (84, 85). Extracellular ROS-dependent chemiluminescence (86) was measured every 5 min for 4h using an SpectraMax i3x microplate reader.

Flow cytometry (conidial phagocytosis, Dectin-1 expression, and intracellular ROS)

For conidial phagocytosis, *A. fumigatus* swollen conidia were labeled using 20 μg/mL Alexa Fluor™ (AF) 488-NHS ester (succinimidyl ester) in PBS for 1h with agitation, rinsed with PBS, and resuspended in FACS buffer (PBS, 2% FBS, 1 mM EDTA). Neutrophils (200,000) in cRPMI

were stimulated with AF488-labeled *A. fumigatus* at MOI 10:1, in a 96-well V-bottom non-treated polypropylene microplate (Corning, Corning, NY, catalog #3357) for 2h at 37°C and 5% CO_2. For Dectin-1 expression, $1x10^6$ neutrophils in cRPMI were incubated with either solvent control (DMSO) or various concentrations of IBT for 4h at 37°C and 5% CO_2. For intracellular ROS production, $1x10^6$ neutrophils in cRPMI were incubated in conical tubes with either DMSO, various concentrations of IBT, or media alone for 4h at 37°C and 5% CO_2. Neutrophils were then moved to FACS tubes, 1μM dihydroethidium (DHR) was added, and then stimulated with 1 mg/mL heat-killed *A. fumigatus* hyphae (B5233 strain), 5 ng/mL PMA, or media alone for 1h at 37°C and 5% CO_2. After stimulation in all experiments, cells were incubated on ice for 10 min. Cells were washed with FACS buffer and treated with Human TruStain FcX, 7-AAD (viability) for phagocytosis and Dectin-1 studies, anti-CD66b-APC, anti-CD45-AF700, and/or anti-Dectin-1-PE (BioLegend, San Diego, CA, catalog #422302, #305118, #304024, and #355404, respectively). Experimental samples were analyzed using a BD FACSCelesta Cell Analyzer (minimum 10,000 viable $CD66b^+$ events) and the BD FACSDiva software, v.10. The gating strategy is outlined in ***Supplemental Figure 9***.

Neutrophil swarming assay

A microarray printing platform (Picospotter PolyPico, Galway, Ireland) was used to print a solution of 0.1% poly-L-lysine (Sigma-Aldrich, St. Louis, MO, catalog #P8920) and ZETAG 8185 targets (BASF, Florham Park, NJ) with 100 μm diameter in 8 × 8 arrays on a 16-well format on ultra-clean glass slides (Fisher Scientific, Waltham, MA) (36). Slides were screened by microscopy for printing accuracy, dried at room temperature for 2h, and assembled into 16 chambers using ProPlate® Multi-Well Chambers (Grace Bio-Labs, Bend, OR, catalog #204860).

Wells were loaded with 50 µL of *A. fumigatus* resting conidia in sterile H_2O, incubated for 10 min with agitation, and thoroughly washed with PBS to remove unbound conidia. Wells were screened by microscopy to ensure appropriate patterning of targets onto the spots. *Aspergillus*-seeded targets were located using the Nikon Perfect Focus system and multipoint function. Wells were loaded with 500,000 neutrophils stained with 4 µM Hoechst (Thermo Scientific, Waltham, MA, catalog #H3570) in 200 µL of swarming media (Iscove's Modified Dulbecco's Media with 20% FBS). When using chemical inhibitors and cytokines, neutrophils were pre-incubated as described above in swarming media. Live-cell imaging was conducted using a Nikon Ti-E inverted microscope. An excitation light source, 4-W laser (Coherent), was used to produce excitation wavelengths of 405 and 488 nm using an acoustic optical tunable tuner. To acquire differential interference contrast images, a polarizer (MEN 51941; Nikon, Tokyo, Japan) and Wollaston prisms (MBH76190; Nikon, Tokyo, Japan) were used. Images were collected using a 10x objective and an EM-CCD camera (C9100-13; Hamamatsu, Shizuoka, Japan). Image acquisition was performed using MetaMorph 7.10 (Molecular Devices, San Jose, CA). Image analysis was performed using Fiji (87) as described by Hopke et al (36, 88), and raw image data files were processed using Adobe Photoshop 2023.

RNA extraction and qPCR

Neutrophils (400,000) were incubated at 37°C and 5% CO_2 in the presence or absence of *A. fumigatus* (MOI:2.5). After 6h, cells were centrifuged for 5 min at 500 x g and supernatants removed. Cell pellets were resuspended in 350 µL of Buffer RLT containing 1% β-mercaptoethanol and incubated on ice for 10 min. Lysates were homogenized using QIAshredder columns (Qiagen, Hilden, Germany, catalog #79656). Homogenized lysates were mixed with

RNase-free 70% ethanol and purified using the RNeasy Mini Kit (Qiagen, Hilden, Germany, catalog #74134) according to the manufacturer's instructions. RNA concentrations were measured using a NanoDrop™ One (Thermo Scientific, Waltham, MA, catalog #ND-ONE-W) and 1% agarose gels were used to verify RNA integrity.

RNA samples were treated with ezDNase enzyme (Invitrogen). For cDNA synthesis, 15 ng of RNA were combined with the SuperScript IV VILO Master Mix kit (Invitrogen) according to the manufacturer instructions. Reverse transcription was performed for 10 min at 50°C. mRNA was quantified for *CXCL8* (TaqMan Gene Expression Assays, Hs00174103_m1) and the housekeeping gene *GAPDH* (TaqMan Gene Expression Assays, Hs02758991_g1) by quantitative PCR using TaqMAN Fast Advanced Master Mix (Applied Biosystems, Waltham, MA, catalog #4444557) using 2 µL of cDNA in 20 µL reactions, with 40 cycles of 3s at 95°C followed by 30 sec at 60°C (Applied Biosystems™ 7500 Fast Real-Time PCR). Transcript levels were normalized using *GAPDH*.

NanoString nCounter analysis

Transcriptional profiling was obtained using the nCounter® Human Host Response panel (NanoString Technologies, Seattle, WA, catalog #Q-21898) according to the manufacturer's instructions. Briefly, 25 ng of total RNA were used for hybridization reactions at 65°C for 22h, loaded onto a Sprint cartridge, and analyzed using an nCounter SPRINT Profiler (NanoString Technologies, Seattle, WA). Data analysis was performed using nSolver® 4.0. To adjust for differences in total RNA per lane, hybridization efficiency, and post-hybridization processing, the counts of 773 target RNAs were normalized based on negative controls (background subtraction) and the geometric mean of 12 positive control RNA counts.

ELISA

Neutrophils (2,000,000) were treated for 4h with 0.3 μM IBT or DMSO and incubated for 5h at 37°C and 5% CO_2 in the presence or absence of *A. fumigatus* (MOI:2.5). TNFα from the supernatant was measured using the ELISA MAX Deluxe Set (BioLegend, San Diego, CA, catalog #430204) following the manufacturer's instructions.

Statistics

Statistical analysis was performed using GraphPad Prism 9 software for all studies except for NanoString studies, which was performed using nSolver® Advance Analysis 2.0. Data is presented as mean ± SD or percentage ± 95% CI. For extracellular ROS production studies, the area under the curve (AUC) was calculated. For all studies except for NanoString experiments, statistical differences were obtained using an ordinary one-way ANOVA and Tukey's multiple comparisons test with a single pooled variance. A p-value ≤ 0.05 was considered significant. For NanoSting studies, the fold changes, p-values, and adjusted p-values were obtained using the Benjamini-Yekutieli method. Only genes with an adjusted p-value ≤ 0.05 and a $\log_2$ fold-change of ± 1.5 were significant.

Study Approval

The use of human blood samples to isolate primary neutrophils was approved by the Institutional Review Board at Massachusetts General Hospital (Protocol #2015P000818). Informed consent for data used was provided by all participants prior to participation in the study.

Data Availability

NanoString raw data files and normalized data are available through the GEO database (Accension Number: GSE264298). Raw data for figures presented in this manuscript are available in the Supporting Data Values XLS file.

AUTHOR CONTRIBUTIONS

D.A.V.-B., O.W.H., A.H., and J.M.V. conceptualized the study and developed the methodology; D.A.V.-B., O.W.H., K.J.B., P.S., A.J.C, K.D.T., A.H., H.E.B., K.N.J., D.J.F., J.L.R., and C.R. performed experiments; D.A.V.-B., O.W.H., K.J.B., A.H., S.R.V., and J.M.V., analyzed and interpreted data; D.A.V.-B., K.J.B., C.R., R.A.W., J.S.A., and J.M.V. coordinated and managed experiments using clinical samples; D.A.V.-B., O.W.H., R.A.W., and J.M.V. drafted the paper; D.A.V.-B., O.W.H., K.J.B., P.S., A.J.C., K.D.T., A.H., H.E.B., S.R.V., K.N.J., D.J.F., J.L.R., C.R., M.K.M., R.A.W., D.I., J.S.A., and J.M.V. reviewed and edited the paper. D.A.V.-B performed most of the experiments and is listed as the first author of the first co-authors.

ACKNOWLEDGEMENTS

This work was supported by the National Institutes of Health (NIH) grants R01AI150181, R01AI136529, and R21AI152499 (J.M.V.), NIH/NIAID grant K08AI14755 (J.L.R.), R01AI132638 (M.K.M.), R01AI176658 (D.I. and M.K.M.), R01GM092804 (D.I.), and the MGH Fund for Medical Discovery Research Fellowship award (H.B.H). We thank all members of the Mansour laboratory, Tanya Mayadas, and Cliff Lowell for technical assistance and helpful discussions. Furthermore, we thank Nicole Wolf for assistance with the artwork. Illustration (graphical abstract) by Nicole Wolf, MS, ©2022. Printed with permission.

Conflict-of-interest disclosure

The authors declare no competing financial interests.

REFERENCES

1. Gregg KS, and Kauffman CA. Invasive aspergillosis: epidemiology, clinical aspects, and treatment. *Semin Respir Crit Care Med.* 2015;36(5):662-72.
2. Pagano L, Caira M, Candoni A, Offidani M, Martino B, Specchia G, et al. Invasive aspergillosis in patients with acute myeloid leukemia: a SEIFEM-2008 registry study. *Haematologica.* 2010;95(4):644-50.
3. Nucci M, Garnica M, Gloria AB, Lehugeur DS, Dias VC, Palma LC, et al. Invasive fungal diseases in haematopoietic cell transplant recipients and in patients with acute myeloid leukaemia or myelodysplasia in Brazil. *Clin Microbiol Infect.* 2013;19(8):745-51.
4. Colombo AL, Bergamasco MD, Nouer SA, Oliveira ECPT, Pasqualotto AC, de Queiroz-Telles F, et al. Invasive aspergillosis in patients with acute leukemia: comparison between acute myeloid and acute lymphoid leukemia. *Mycopathologia.* 2022.
5. Desai JV, and Lionakis MS. The role of neutrophils in host defense against invasive fungal infections. *Curr Clin Microbiol Rep.* 2018;5(3):181-9.
6. Margalit A, and Kavanagh K. The innate immune response to *Aspergillus fumigatus* at the alveolar surface. *FEMS Microbiol Rev.* 2015;39(5):670-87.
7. Negoro PE, Xu S, Dagher Z, Hopke A, Reedy JL, Feldman MB, et al. Spleen tyrosine kinase is a critical regulator of neutrophil responses to *Candida* species. *mBio.* 2020;11(3):e02043-19.
8. Nasillo V, Lagreca I, Vallerini D, Barozzi P, Riva G, Maccaferri M, et al. BTK inhibitors impair platelet-mediated antifungal activity. *Cells.* 2022;11(6):1003.
9. Strijbis K, Tafesse FG, Fairn GD, Witte MD, Dougan SK, Watson N, et al. Bruton's tyrosine kinase (BTK) and Vav1 contribute to Dectin1-dependent phagocytosis of *Candida albicans* in macrophages. *PLoS Pathog.* 2013;9(6):e1003446.
10. Becker KL, Aimanianda V, Wang X, Gresnigt MS, Ammerdorffer A, Jacobs CW, et al. *Aspergillus* cell wall chitin induces anti- and proinflammatory cytokines in human PBMCs via the Fc-γ receptor/Syk/PI3K pathway. *mBio.* 2016;7(3):e01823-15.

11. Höft MA, Hoving JC, and Brown GD. Signaling C-type lectin receptors in antifungal immunity. *Curr Top Microbiol Immunol.* 2020;429:63-101.
12. Weber ANR, Bittner Z, Liu X, Dang TM, Radsak MP, and Brunner C. Bruton's tyrosine kinase: an emerging key player in innate immunity. *Front Immunol.* 2017;8:1454.
13. Honigberg LA, Smith AM, Sirisawad M, Verner E, Loury D, Chang B, et al. The Bruton tyrosine kinase inhibitor PCI-32765 blocks B-cell activation and is efficacious in models of autoimmune disease and B-cell malignancy. *Proc Natl Acad Sci U S A.* 2010;107(29):13075-80.
14. Itchaki G, and Brown JR. Experience with ibrutinib for first-line use in patients with chronic lymphocytic leukemia. *Ther Adv Hematol.* 2018;9(1):3-19.
15. Lionakis MS, Dunleavy K, Roschewski M, Widemann BC, Butman JA, Schmitz R, et al. Inhibition of B cell receptor signaling by ibrutinib in primary CNS lymphoma. *Cancer Cell.* 2017;31(6):833-43 e5.
16. Wilson WH, Young RM, Schmitz R, Yang Y, Pittaluga S, Wright G, et al. Targeting B cell receptor signaling with ibrutinib in diffuse large B cell lymphoma. *Nat Med.* 2015;21(8):922-6.
17. Bonnett CR, Cornish EJ, Harmsen AG, and Burritt JB. Early neutrophil recruitment and aggregation in the murine lung inhibit germination of *Aspergillus fumigatus* conidia. *Infect Immun.* 2006;74(12):6528-39.
18. Blez D, Blaize M, Soussain C, Boissonnas A, Meghraoui-Kheddar A, Menezes N, et al. Ibrutinib induces multiple functional defects in the neutrophil response against *Aspergillus fumigatus*. *Haematologica.* 2020;105(2):478-89.
19. Risnik D, Elias EE, Keitelman I, Colado A, Podaza E, Cordini G, et al. The effect of ibrutinib on neutrophil and gammadelta T cell functions. *Leuk Lymphoma.* 2020;61(10):2409-18.
20. Ghez D, Calleja A, Protin C, Baron M, Ledoux MP, Damaj G, et al. Early-onset invasive aspergillosis and other fungal infections in patients treated with ibrutinib. *Blood.* 2018;131(17):1955-9.
21. Fernandes MJ, Lachance G, Pare G, Rollet-Labelle E, and Naccache PH. Signaling through CD16b in human neutrophils involves the Tec family of tyrosine kinases. *J Leukoc Biol.* 2005;78(2):524-32.

22. Gilbert C, Levasseur S, Desaulniers P, Dusseault AA, Thibault N, Bourgoin SG, et al. Chemotactic factor-induced recruitment and activation of Tec family kinases in human neutrophils. II. Effects of LFM-A13, a specific Btk inhibitor. *J Immunol.* 2003;170(10):5235-43.
23. Lachance G, Levasseur S, and Naccache PH. Chemotactic factor-induced recruitment and activation of Tec family kinases in human neutrophils. Implication of phosphatidynositol 3-kinases. *J Biol Chem.* 2002;277(24):21537-41.
24. Melcher M, Unger B, Schmidt U, Rajantie IA, Alitalo K, and Ellmeier W. Essential roles for the Tec family kinases Tec and Btk in M-CSF receptor signaling pathways that regulate macrophage survival. *J Immunol.* 2008;180(12):8048-56.
25. Bercusson A, Colley T, Shah A, Warris A, and Armstrong-James D. Ibrutinib blocks Btk-dependent NF-kB and NFAT responses in human macrophages during *Aspergillus fumigatus* phagocytosis. *Blood.* 2018;132(18):1985-8.
26. Colado A, Genoula M, Cougoule C, Marin Franco JL, Almejun MB, Risnik D, et al. Effect of the BTK inhibitor ibrutinib on macrophage- and gammadelta T cell-mediated response against *Mycobacterium tuberculosis*. *Blood Cancer J.* 2018;8(11):100.
27. Colado A, Marín Franco JL, Elías EE, Amondarain M, Vergara Rubio M, Sarapura Martínez V, et al. Second generation BTK inhibitors impair the anti-fungal response of macrophages and neutrophils. *Am J Hematol.* 2020;95(7):E174-e8.
28. de Porto AP, Liu Z, de Beer R, Florquin S, de Boer OJ, Hendriks RW, et al. Btk inhibitor ibrutinib reduces inflammatory myeloid cell responses in the lung during murine pneumococcal pneumonia. *Mol Med.* 2019;25(1):3.
29. Fiorcari S, Maffei R, Audrito V, Martinelli S, Ten Hacken E, Zucchini P, et al. Ibrutinib modifies the function of monocyte/macrophage population in chronic lymphocytic leukemia. *Oncotarget.* 2016;7(40):65968-81.

30. Prezzo A, Cavaliere FM, Bilotta C, Pentimalli TM, Iacobini M, Cesini L, et al. Ibrutinib-based therapy impaired neutrophils microbicidal activity in patients with chronic lymphocytic leukemia during the early phases of treatment. *Leuk Res.* 2019;87:106233.
31. Stadler N, Hasibeder A, Lopez PA, Teschner D, Desuki A, Kriege O, et al. The Bruton tyrosine kinase inhibitor ibrutinib abrogates triggering receptor on myeloid cells 1-mediated neutrophil activation. *Haematologica.* 2017;102(5):e191-e4.
32. Fiorcari S, Maffei R, Vallerini D, Scarfò L, Barozzi P, Maccaferri M, et al. BTK inhibition impairs the innate response against fungal infection in patients with chronic lymphocytic leukemia. *Front Immunol.* 2020;11:2158.
33. Guo R, Yan Z, Liao H, Guo D, Tao R, Yu X, et al. Ibrutinib suppresses the activation of neutrophils and macrophages and exerts therapeutic effect on acute peritonitis induced by zymosan. *Int Immunopharmacol.* 2022;113(Pt B):109469.
34. Advani RH, Buggy JJ, Sharman JP, Smith SM, Boyd TE, Grant B, et al. Bruton tyrosine kinase inhibitor ibrutinib (PCI-32765) has significant activity in patients with relapsed/refractory B-cell malignancies. *J Clin Oncol.* 2013;31(1):88-94.
35. Rubin-Bejerano I, Abeijon C, Magnelli P, Grisafi P, and Fink GR. Phagocytosis by human neutrophils is stimulated by a unique fungal cell wall component. *Cell Host Microbe.* 2007;2(1):55-67.
36. Hopke A, Scherer A, Kreuzburg S, Abers MS, Zerbe CS, Dinauer MC, et al. Neutrophil swarming delays the growth of clusters of pathogenic fungi. *Nat Commun.* 2020;11(1):2031.
37. Huang X, Chen Y, Chung CS, Yuan Z, Monaghan SF, Wang F, et al. Identification of B7-H1 as a novel mediator of the innate immune/proinflammatory response as well as a possible myeloid cell prognostic biomarker in sepsis. *J Immunol.* 2014;192(3):1091-9.
38. Seo SK, Jeong HY, Park SG, Lee SW, Choi IW, Chen L, et al. Blockade of endogenous B7-H1 suppresses antibacterial protection after primary *Listeria* monocytogenes infection. *Immunology.* 2008;123(1):90-9.

39. Abdel-Latif D, Steward M, Macdonald DL, Francis GA, Dinauer MC, and Lacy P. Rac2 is critical for neutrophil primary granule exocytosis. *Blood.* 2004;104(3):832-9.
40. Blaser H, Dostert C, Mak TW, and Brenner D. TNF and ROS crosstalk in inflammation. *Trends Cell Biol.* 2016;26(4):249-61.
41. Desai JV, Zarakas MA, Wishart AL, Roschewski M, Aufiero MA, Donkò A, et al. BTK drives neutrophil activation for sterilizing antifungal immunity *J Clin Invest.* 2024;*In revision*.
42. Awan FT, Schuh A, Brown JR, Furman RR, Pagel JM, Hillmen P, et al. Acalabrutinib monotherapy in patients with chronic lymphocytic leukemia who are intolerant to ibrutinib. *Blood Adv.* 2019;3(9):1553-62.
43. Alkharabsheh O, Alsayed A, Morlote DM, and Mehta A. Cerebral invasive aspergillosis in a case of chronic lymphocytic leukemia with Bruton tyrosine kinase inhibitor. *Curr Oncol.* 2021;28(1):837-41.
44. Patel D, Sidana M, Mdluli X, Patel V, Stapleton A, and Dasanu CA. A fatal disseminated cryptococcal infection in a patient treated with zanubrutinib for Waldenstrom's macroglobulinemia. *J Oncol Pharm Pract.* 2022;28(8):1917-21.
45. Tam CS, Opat S, Simpson D, Cull G, Munoz J, Phillips TJ, et al. Zanubrutinib for the treatment of relapsed or refractory mantle cell lymphoma. *Blood Adv.* 2021;5(12):2577-85.
46. Tam CS, Dimopoulos M, Garcia-Sanz R, Trotman J, Opat S, Roberts AW, et al. Pooled safety analysis of zanubrutinib monotherapy in patients with B-cell malignancies. *Blood Adv.* 2022;6(4):1296-308.
47. Tam CS, Ou YC, Trotman J, and Opat S. Clinical pharmacology and PK/PD translation of the second-generation Bruton's tyrosine kinase inhibitor, zanubrutinib. *Expert Rev Clin Pharmacol.* 2021;14(11):1329-44.
48. Estupinan HY, Berglof A, Zain R, and Smith CIE. Comparative analysis of BTK inhibitors and mechanisms underlying adverse effects. *Front Cell Dev Biol.* 2021;9:630942.

49. Xu Y, Izumi R, Nguyen H, Kwan A, Kuo H, Madere J, et al. Evaluation of the pharmacokinetics and safety of a single dose of acalabrutinib in subjects with hepatic impairment. *J Clin Pharmacol.* 2022;62(6):812-22.
50. Tam CS, Trotman J, Opat S, Burger JA, Cull G, Gottlieb D, et al. Phase 1 study of the selective BTK inhibitor zanubrutinib in B-cell malignancies and safety and efficacy evaluation in CLL. *Blood.* 2019;134(11):851-9.
51. Ou YC, Liu L, Tariq B, Wang K, Jindal A, Tang Z, et al. Population pharmacokinetic analysis of the BTK inhibitor zanubrutinib in healthy volunteers and patients with B-cell malignancies. *Clin Transl Sci.* 2021;14(2):764-72.
52. Zhang Y, Li Y, Zhuang Z, Wang W, Wei C, Zhao D, et al. Preliminary evaluation of zanubrutinib-containing regimens in DLBCL and the cerebrospinal fluid distribution of zanubrutinib: a 13-case series. *Front Oncol.* 2021;11:760405.
53. Sollberger G, Amulic B, and Zychlinsky A. Neutrophil extracellular trap formation is independent of de novo gene expression. *PLoS One.* 2016;11(6):e0157454.
54. Patin EC, Thompson A, and Orr SJ. Pattern recognition receptors in fungal immunity. *Semin Cell Dev Biol.* 2019;89:24-33.
55. Ward RA, and Vyas JM. The first line of defense: effector pathways of anti-fungal innate immunity. *Curr Opin Microbiol.* 2020;58:160-5.
56. van Bruggen R, Drewniak A, Jansen M, van Houdt M, Roos D, Chapel H, et al. Complement receptor 3, not Dectin-1, is the major receptor on human neutrophils for beta-glucan-bearing particles. *Mol Immunol.* 2009;47(2-3):575-81.
57. Taylor PR, Tsoni SV, Willment JA, Dennehy KM, Rosas M, Findon H, et al. Dectin-1 is required for β-glucan recognition and control of fungal infection. *Nature Immunology.* 2007;8(1):31-8.
58. Lo SK, Lee S, Ramos RA, Lobb R, Rosa M, Chi-Rosso G, et al. Endothelial-leukocyte adhesion molecule 1 stimulates the adhesive activity of leukocyte integrin CR3 (CD11b/CD18, Mac-1, alpha m beta 2) on human neutrophils. *J Exp Med.* 1991;173(6):1493-500.

59. Evans R, Patzak I, Svensson L, De Filippo K, Jones K, McDowall A, et al. Integrins in immunity. *J Cell Sci.* 2009;122(Pt 2):215-25.
60. Abram CL, and Lowell CA. The ins and outs of leukocyte integrin signaling. *Annu Rev Immunol.* 2009;27:339-62.
61. Basoni C, Nobles M, Grimshaw A, Desgranges C, Davies D, Perretti M, et al. Inhibitory control of TGF-beta1 on the activation of Rap1, CD11b, and transendothelial migration of leukocytes. *FASEB J.* 2005;19(7):822-4.
62. Futosi K, Fodor S, and Mocsai A. Neutrophil cell surface receptors and their intracellular signal transduction pathways. *Int Immunopharmacol.* 2013;17(3):638-50.
63. Volmering S, Block H, Boras M, Lowell CA, and Zarbock A. The neutrophil Btk signalosome regulates integrin activation during sterile inflammation. *Immunity.* 2016;44(1):73-87.
64. Herbst S, Shah A, Mazon Moya M, Marzola V, Jensen B, Reed A, et al. Phagocytosis-dependent activation of a TLR9-BTK-calcineurin-NFAT pathway co-ordinates innate immunity to *Aspergillus fumigatus*. *EMBO Mol Med.* 2015;7(3):240-58.
65. Marciano BE, Spalding C, Fitzgerald A, Mann D, Brown T, Osgood S, et al. Common severe infections in chronic granulomatous disease. *Clin Infect Dis.* 2015;60(8):1176-83.
66. Blumental S, Mouy R, Mahlaoui N, Bougnoux ME, Debré M, Beauté J, et al. Invasive mold infections in chronic granulomatous disease: a 25-year retrospective survey. *Clin Infect Dis.* 2011;53(12):e159-69.
67. Ruchlemer R, Ben-Ami R, Bar-Meir M, Brown JR, Malphettes M, Mous R, et al. Ibrutinib-associated invasive fungal diseases in patients with chronic lymphocytic leukaemia and non-Hodgkin lymphoma: An observational study. *Mycoses.* 2019;62(12):1140-7.
68. Varughese T, Taur Y, Cohen N, Palomba ML, Seo SK, Hohl TM, et al. Serious infections in patients receiving ibrutinib for treatment of lymphoid cancer. *Clin Infect Dis.* 2018;67(5):687-92.

69. Nam HY, Nam JH, Yoon G, Lee JY, Nam Y, Kang HJ, et al. Ibrutinib suppresses LPS-induced neuroinflammatory responses in BV2 microglial cells and wild-type mice. *J Neuroinflammation.* 2018;15(1):271.
70. Sullivan BN, Baggett MA, Guillory C, Jones M, and Steele C. Neuroimmune responses in a new experimental animal model of cerebral aspergillosis. *mBio.* 2022;13(5):e0225422.
71. Jang DI, Lee AH, Shin HY, Song HR, Park JH, Kang TB, et al. The role of tumor necrosis factor alpha (TNF-α) in autoimmune disease and current TNF-α inhibitors in therapeutics. *Int J Mol Sci.* 2021;22(5):2719.
72. Keaney J, Gasser J, Gillet G, Scholz D, and Kadiu I. Inhibition of Bruton's tyrosine kinase modulates microglial phagocytosis: therapeutic implications for Alzheimer's disease. *J Neuroimmune Pharmacol.* 2019;14(3):448-61.
73. van Loo G, and Bertrand MJM. Death by TNF: a road to inflammation. *Nat Rev Immunol.* 2022;23(5):289-303.
74. Ramos-Casals M, Brito-Zeron P, Munoz S, Soria N, Galiana D, Bertolaccini L, et al. Autoimmune diseases induced by TNF-targeted therapies: analysis of 233 cases. *Medicine (Baltimore).* 2007;86(4):242-51.
75. Ordonez ME, Farraye FA, and Di Palma JA. Endemic fungal infections in inflammatory bowel disease associated with anti-TNF antibody therapy. *Inflamm Bowel Dis.* 2013;19(11):2490-500.
76. Tragiannidis A, Kyriakidis I, Zündorf I, and Groll AH. Invasive fungal infections in pediatric patients treated with tumor necrosis alpha (TNF-α) inhibitors. *Mycoses.* 2017;60(4):222-9.
77. Tsai HF, Washburn RG, Chang YC, and Kwon-Chung KJ. *Aspergillus fumigatus* arp1 modulates conidial pigmentation and complement deposition. *Mol Microbiol.* 1997;26(1):175-83.
78. Pain A, Woodward J, Quail MA, Anderson MJ, Clark R, Collins M, et al. Insight into the genome of *Aspergillus fumigatus*: analysis of a 922 kb region encompassing the nitrate assimilation gene cluster. *Fungal Genet Biol.* 2004;41(4):443-53.

79. Hearn VM, and Mackenzie DW. Mycelial antigens from two strains of *Aspergillus fumigatus*: an analysis by two-dimensional immunoelectrophoresis. *Mykosen.* 1980;23(10):549-62.
80. Girardin H, Latge JP, Srikantha T, Morrow B, and Soll DR. Development of DNA probes for fingerprinting *Aspergillus fumigatus*. *J Clin Microbiol.* 1993;31(6):1547-54.
81. Monod M, Paris S, Sarfati J, Jaton-Ogay K, Ave P, and Latge JP. Virulence of alkaline protease-deficient mutants of *Aspergillus fumigatus*. *FEMS Microbiol Lett.* 1993;106(1):39-46.
82. Reedy JL, Crossen AJ, Negoro PE, Harding HB, Ward RA, Vargas-Blanco DA, et al. The C-type lectin receptor Dectin-2 is a receptor for *Aspergillus fumigatus* galactomannan. *mBio.* 2023;14(1):e0318422.
83. Tam JM, Mansour MK, Khan NS, Yoder NC, and Vyas JM. Use of fungal derived polysaccharide-conjugated particles to probe Dectin-1 responses in innate immunity. *Integr Biol (Camb).* 2012;4(2):220-7.
84. Gyllenhammar H. Lucigenin chemiluminescence in the assessment of neutrophil superoxide production. *J Immunol Methods.* 1987;97(2):209-13.
85. Briheim G, Stendahl O, and Dahlgren C. Intra- and extracellular events in luminol-dependent chemiluminescence of polymorphonuclear leukocytes. *Infect Immun.* 1984;45(1):1-5.
86. Caldefie-Chezet F, Walrand S, Moinard C, Tridon A, Chassagne J, and Vasson MP. Is the neutrophil reactive oxygen species production measured by luminol and lucigenin chemiluminescence intra or extracellular? Comparison with DCFH-DA flow cytometry and cytochrome c reduction. *Clin Chim Acta.* 2002;319(1):9-17.
87. Schindelin J, Arganda-Carreras I, Frise E, Kaynig V, Longair M, Pietzsch T, et al. Fiji: an open-source platform for biological-image analysis. *Nat Methods.* 2012;9(7):676-82.
88. Hopke A, and Irimia D. Ex Vivo Human Neutrophil Swarming Against Live Microbial Targets. *Methods Mol Biol.* 2020;2087:107-16.

FIGURES

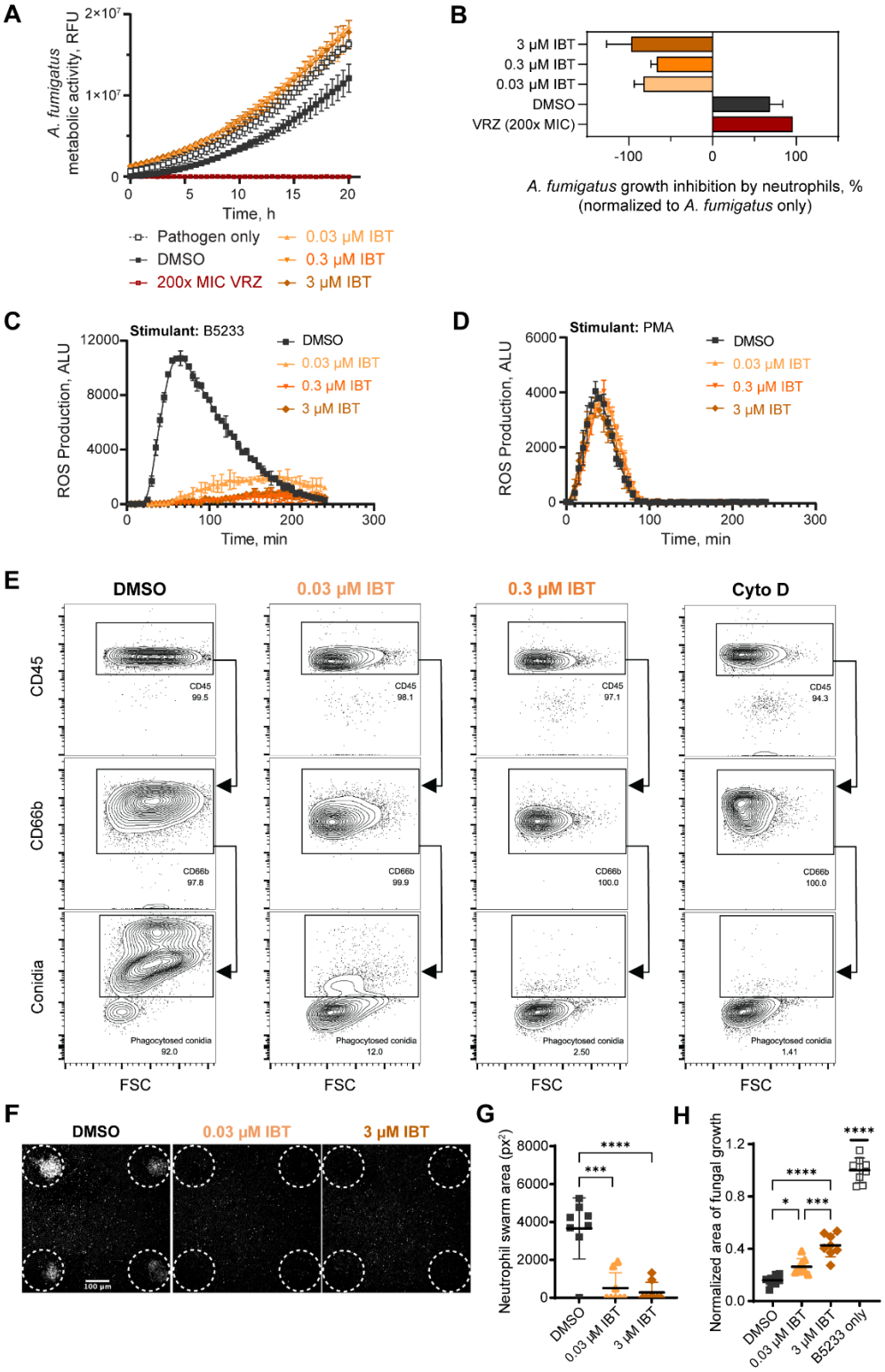

Figure 1. IBT inhibition dampened human neutrophil effector activity against *A. fumigatus*. **(A)** Metabolic activity of *A. fumigatus* B5233 strain measured using resazurin. Human neutrophils

were pretreated for 4h with IBT and stimulated with *A. fumigatus* (MOI:0.25) for 5h. Error bars are SD, $n = 3$, data representative of at least three independent experiments. **(B)** Percentages of growth inhibition derived from (A) using linear regression analysis in a Gompertz fit. Error bars are 95% CI, $n = 3$. Ordinary one-way ANOVA and Tukey's multiple comparisons test with a single pooled variance demonstrated a p-value < 0.0001 for all IBT treatments vs DMSO alone. **(C, D)** Human neutrophils were treated for 4h with IBT or DMSO and then stimulated with 1 mg/mL *A. fumigatus* B5233 strain heat-killed hyphal elements (C) or 1 µg/mL PMA (D). ROS production was measured by chemiluminescence using lucigenin. Error bars are SD, $n = 3$. **(E)** Human neutrophils were treated with IBT or DMSO for 4h and incubated with Af488-labeled *A. fumigatus* B5233 strain (conidia$^+$) swollen spores (MOI: 10). A subset of neutrophils was pre-treated with 20 µM of cytochalasin D (CytoD). The displayed percentage of phagocytic neutrophils (CD45-AF700$^+$/CD66b-APC$^+$/conidia-AF488$^+$) was estimated based on the total number of viable neutrophils (CD45-AF700$^+$/CD66b-APC$^+$). A minimum of 10,000 viable CD66b-APC$^+$ events were recorded. **(F, G, H)** Human neutrophils were treated with IBT or DMSO for 4h before co-incubation with *A. fumigatus* B5233 strain. Representative microscopy panels from the swarming assay showing neutrophil swarm formations 200 min after co-incubation, white circles depict areas seeded with *A. fumigatus* (F). Area of human neutrophil swarm 200 min after co-incubation with *A. fumigatus* seeded spores (G). Area of fungal growth per cluster on swarming array slides after 16h, normalized to *A. fumigatus* growth without neutrophils (H). Error bars are SD, $n = 8$. Ordinary one-way ANOVA and Tukey's multiple comparisons test with a single pooled variance, * $p < 0.05$; *** $p < 0.001$; **** $p < 0.0001$. For all panels, data are representative of at least three independent experiments.

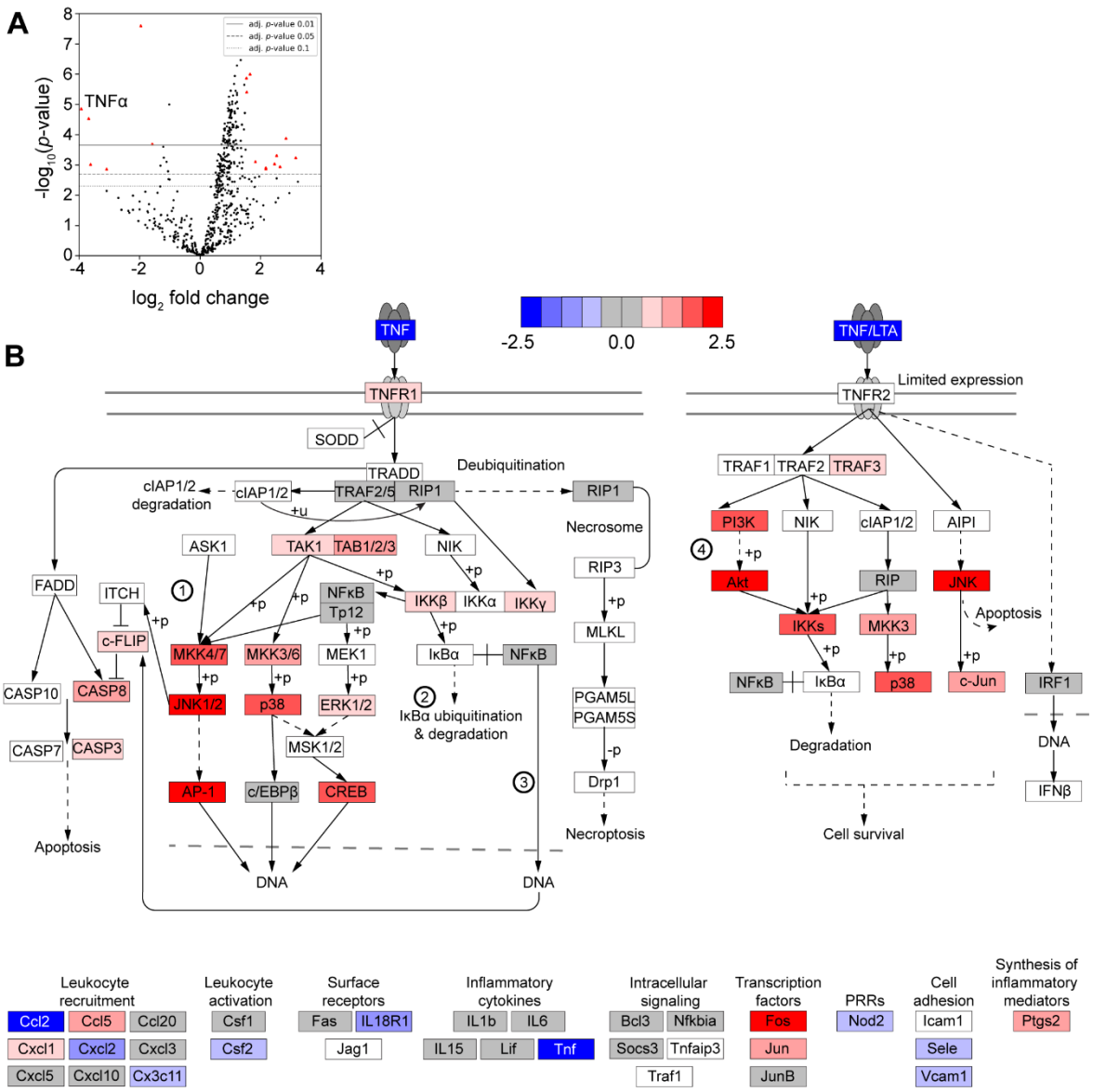

Figure 2. IBT induced downstream upregulation of the TNFα pathway in human neutrophils. (A) Volcano plot for DEGs in neutrophils treated with 0.3 μM IBT vs DMSO (4.5h, unstimulated). DEGs based on $\log_2$ fold change and p-adj < 0.05. FDRs were calculated using the Benjamini-Yekutieli method with three biological replicates per condition. Red and blue dots represent upregulated and downregulated genes, respectively. **(B)** TNFα KEGG pathway was created for all probed genes for IBT-treated neutrophils vs DMSO. Genes in white boxes are genes not included in the nCounter panel. Numbers in circles represent pathways: (1) MAPK signaling pathway; (2) ubiquitin-mediated proteolysis; (3) NFκB signaling pathway; and (4) PI3K-Akt signaling pathway.

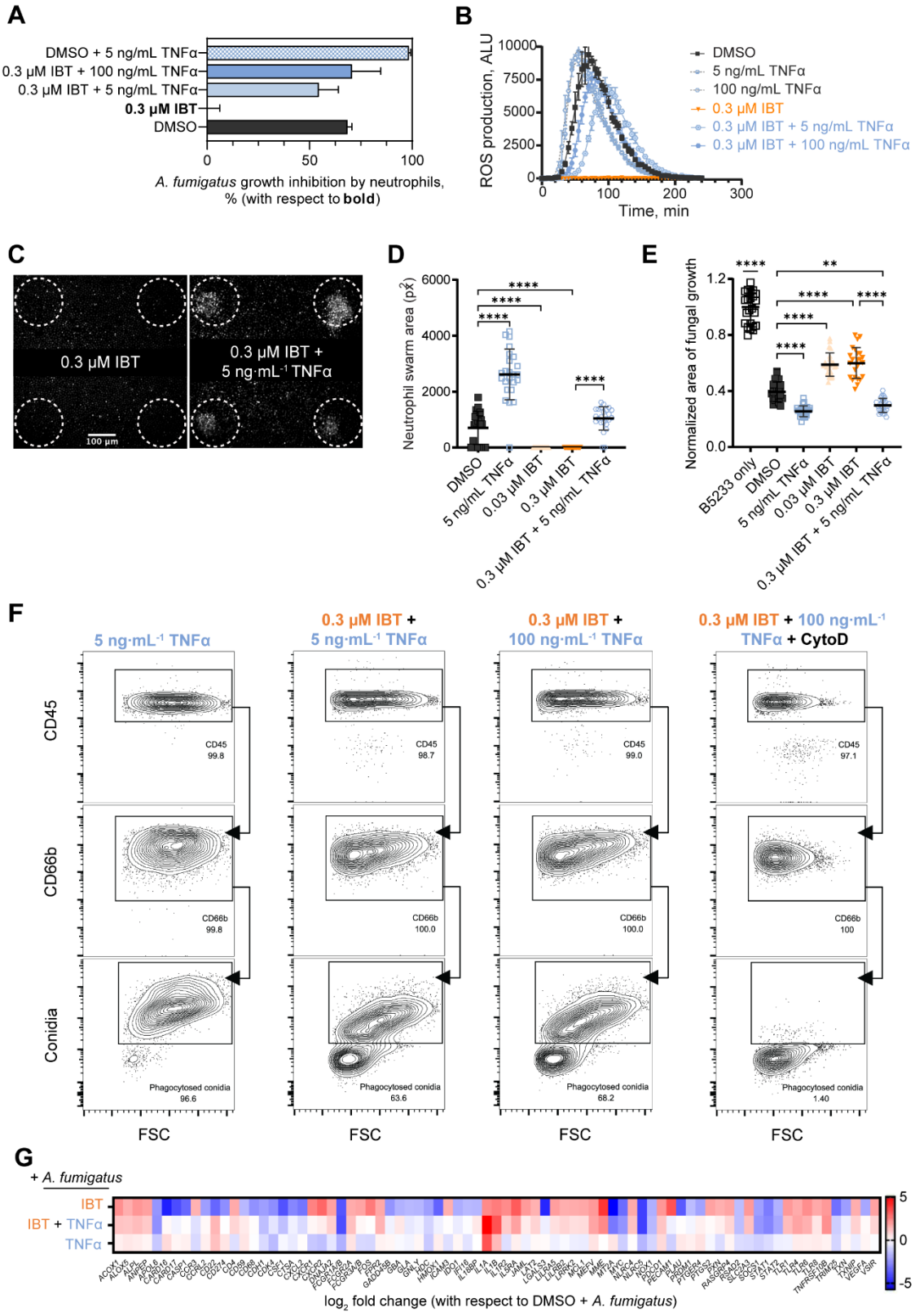

Figure 3. TNFα rescued IBT-induced immune defects in neutrophils against *A. fumigatus*. Human neutrophils were treated with 0.03 μM IBT, 0.3 μM IBT, or DMSO for 30 min followed

by a 4h incubation with TNFα and co-incubated with *A. fumigatus* B5233 strain for all figure panels. For all panels, data are representative of at least three independent experiments. **(A)** Neutrophils were incubated with *A. fumigatus* (MOI:0.25) for 5h and metabolic activity was measured by resazurin assay. Data calculated through time course study (see raw data in Supplemental Materials) and panel represents the output from linear regression analysis using Gompertz fit with percentages of growth inhibition of *A. fumigatus* by neutrophils in reference to IBT-treated neutrophils. Error bars are 95% CI, $n = 3$. Ordinary one-way ANOVA and Tukey's multiple comparisons test with a single pooled variance demonstrated a p-value < 0.001 for all TNFα treatments vs IBT alone. **(B)** Neutrophils were stimulated with 1 mg/mL *A. fumigatus* heat-killed hyphae. ROS production was measured by chemiluminescence using lucigenin. Error bars are SD, $n = 3$. **(C)** Microscopy panels showing neutrophils swarm formations 200 min after co-incubation. **(D)** Area of neutrophil swarm after 200 min. **(E)** Area of fungal growth normalized to the growth of *A. fumigatus* without neutrophils after 16h. Error bars are SD, $n = 24$. Ordinary one-way ANOVA and Tukey's multiple comparisons test with a single pooled variance, ** $p < 0.01$; **** $p < 0.0001$. **(F)** Neutrophils were co-incubated with AF488-labeled *A. fumigatus* swollen spores (MOI: 10). The displayed percentage of phagocytic neutrophils (CD45-AF700$^+$/CD66b-APC$^+$/conidia-AF488$^+$) was estimated based on the total number of viable neutrophils (CD45-AF700$^+$/CD66b-APC$^+$). A minimum of 10,000 viable CD66b-APC$^+$ events were recorded. **(G)** Heatmap for DEG based on $\log_2$ fold change (1.5 < log2 fold change < -1.5) and a p-adj value < 0.05. FDR was calculated using the Benjamini-Yekutieli method with three biological replicates per condition. RNA from neutrophils co-incubated for 5h with *A. fumigatus* B5233 strain (MOI:2.5).

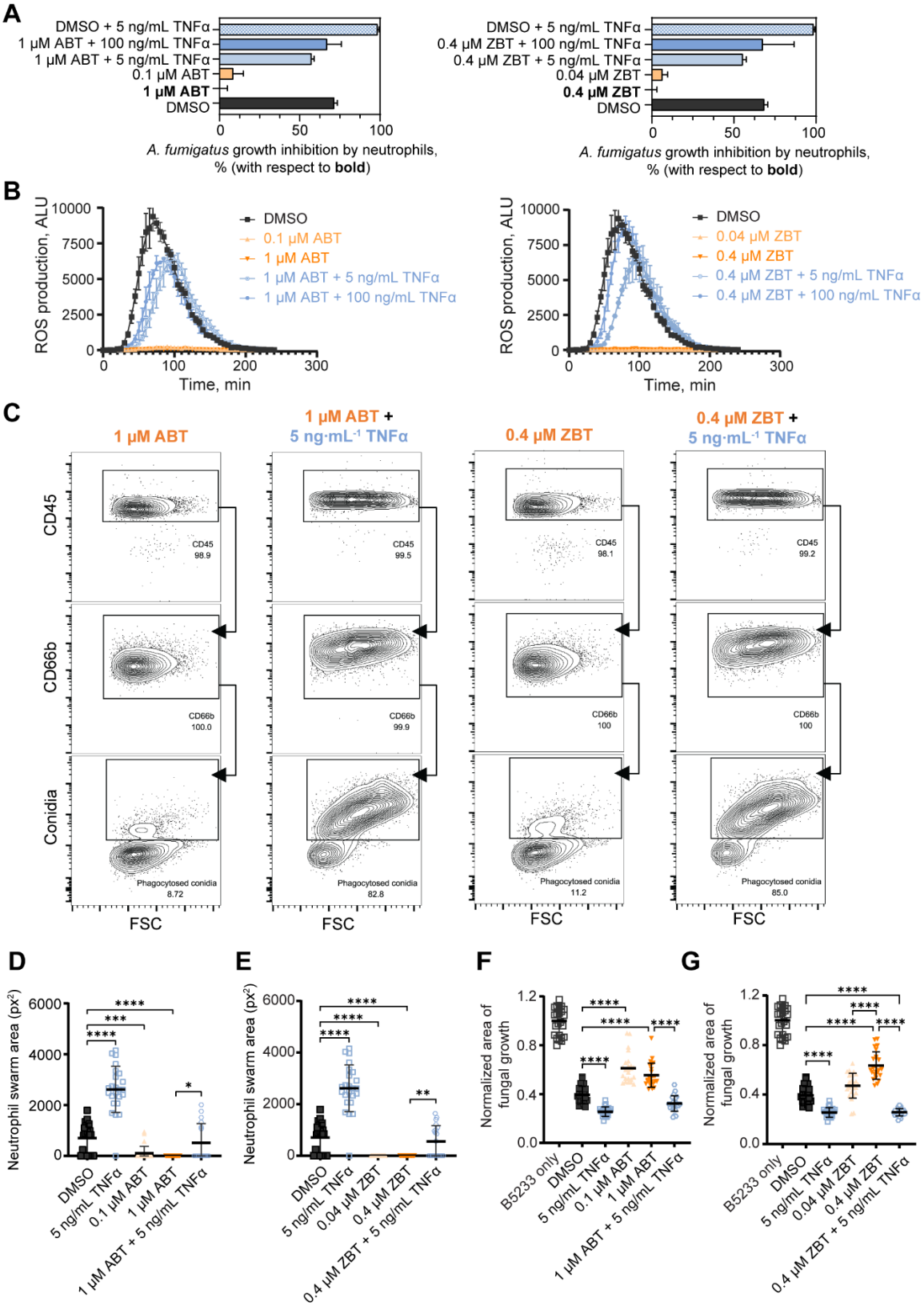

Figure 4. TNFα restored defects caused by multiple BTK inhibitors on neutrophil immune activity against *A. fumigatus*. Human neutrophils were treated with ABT, ZBT, or DMSO for 30

min followed by a 4h incubation with TNFα and co-incubated with *A. fumigatus* B5233 strain for all figure panels. For all panels, data are representative of at least three independent experiments. **(A)** Neutrophils were incubated with *A. fumigatus* (MOI:0.25) for 5h, and metabolic activity was measured using a resazurin assay. Data calculated through time course study (see raw data in Supplemental Materials) and panel represents the output from linear regression analysis using Gompertz fit with percentages of growth inhibition of *A. fumigatus* by neutrophils in reference to neutrophils treated with the respective BTK inhibitor. Error bars are 95% CI, $n = 3$. Ordinary one-way ANOVA and Tukey's multiple comparisons test with a single pooled variance demonstrated a p-value < 0.001 for all IBT treatments vs BTK inhibitor (ABT or ZBT) alone. **(B)** Neutrophils were incubated with 1 mg/mL *A. fumigatus* heat-killed hyphae. ROS production was measured by chemiluminescence using lucigenin. Error bars are SD, $n = 3$. **(C)** Neutrophils treated with ABT (left two panels) or ZBT (right two panels) were co-incubated with labeled *A. fumigatus* swollen spores (MOI: 10). The displayed percentage of phagocytic neutrophils (CD45-AF700$^+$/CD66b-APC$^+$/conidia-AF488$^+$) was estimated based on the total number of viable neutrophils (CD45-AF700$^+$/CD66b-APC$^+$). A minimum of 10,000 viable CD66b-APC$^+$ events were recorded. **(D-G)** Swarming assay was measured by confocal microscopy view of *A. fumigatus* conidia spots after 200 min. Area of neutrophil swarm after 200 min for neutrophils treated with ABT **(D)** or ZBT **(E)**. Area of fungal growth per cluster on swarming array slides normalized to the growth of *A. fumigatus* without neutrophils after 16h, for neutrophils treated with ABT **(F)** or ZBT **(G)**. Treatment controls correspond to the same swarming array experiment (D-G). Error bars are SD, $n = 24$. Ordinary one-way ANOVA and Tukey's multiple comparisons test with a single pooled variance, ** $p < 0.01$; *** $p < 0.001$; **** $p < 0.0001$.

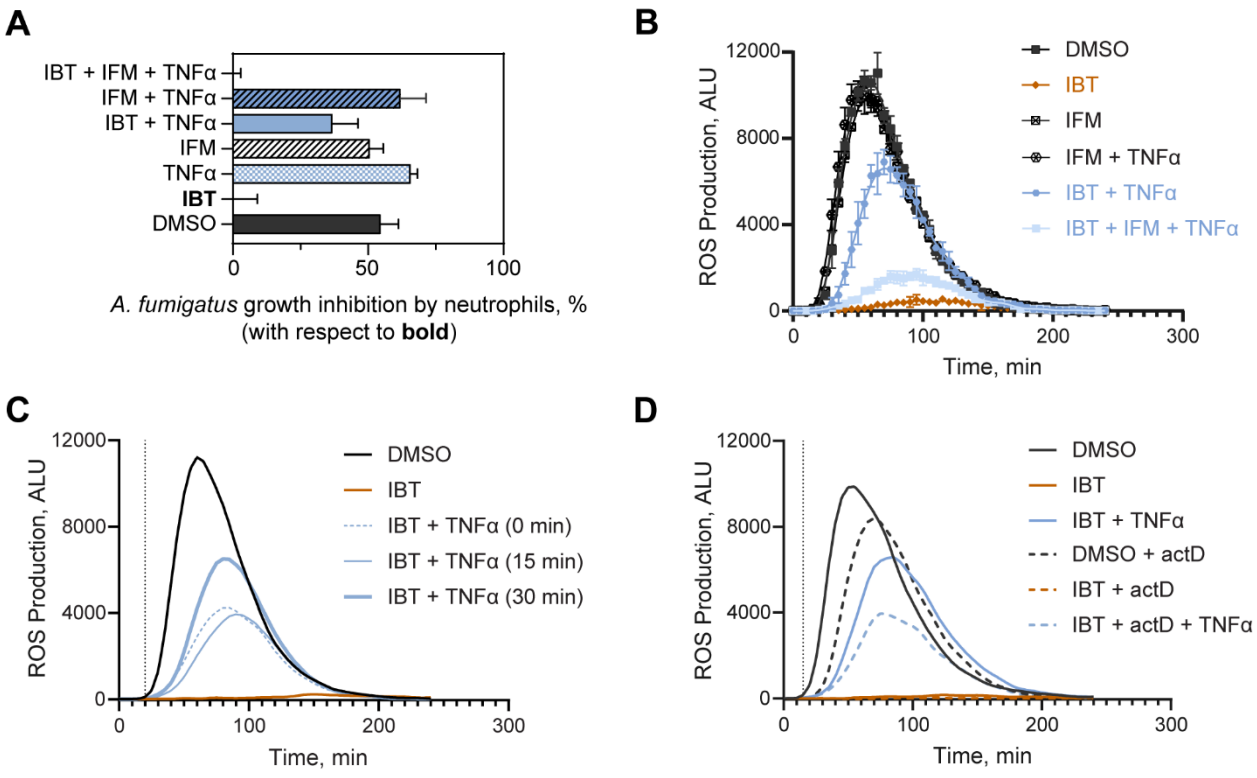

Figure 5. Restorative activity of exogenous TNFα signals independent of transcription. **(A)** Neutrophils were incubated with *A. fumigatus* B5233 strain (MOI:2.5) for 5h and metabolic activity was estimated by fluorescence. Data calculated through time course study (see raw data in Supplemental Materials) and panel represents the output from linear regression analysis using Gompertz fit with Error bars are 95% CI, $n = 3$. Ordinary one-way ANOVA and Tukey's multiple comparisons test with a single pooled variance demonstrated a p-value < 0.001 for TNFα alone, IFM alone, and in combination with IBT treatments vs IBT alone, p-value = 0.0004 for IBT + TNFα vs IBT alone. **(B)** ROS production in IBT-treated neutrophils incubated with 25 µg/mL IFM in the presence of exogenous TNFα and co-incubated with 1 mg/mL *A. fumigatus* heat-killed hyphae. Error bars are SD, $n = 3$, data representative from at least three independent experiments. **(C)** Neutrophils were treated with 0.3 µM IBT for 30 min followed by 5 ng/mL TNFα for the time indicated. To better visualize the starting point of ROS production (black dotted line, 20 min), only the trend but not the time points are shown. **(D)** Neutrophils were treated with DMSO or 0.3 µM IBT for 30 min followed by 1 µg/mL actD for 15 min and by 5 ng/mL TNFα for 1h. ROS production was measured after stimulation with 1 mg/mL *A. fumigatus* heat-killed hyphae. The black dotted line represents the starting point of ROS production (15 min) upon stimulation with *A. fumigatus* for treatments containing actD.

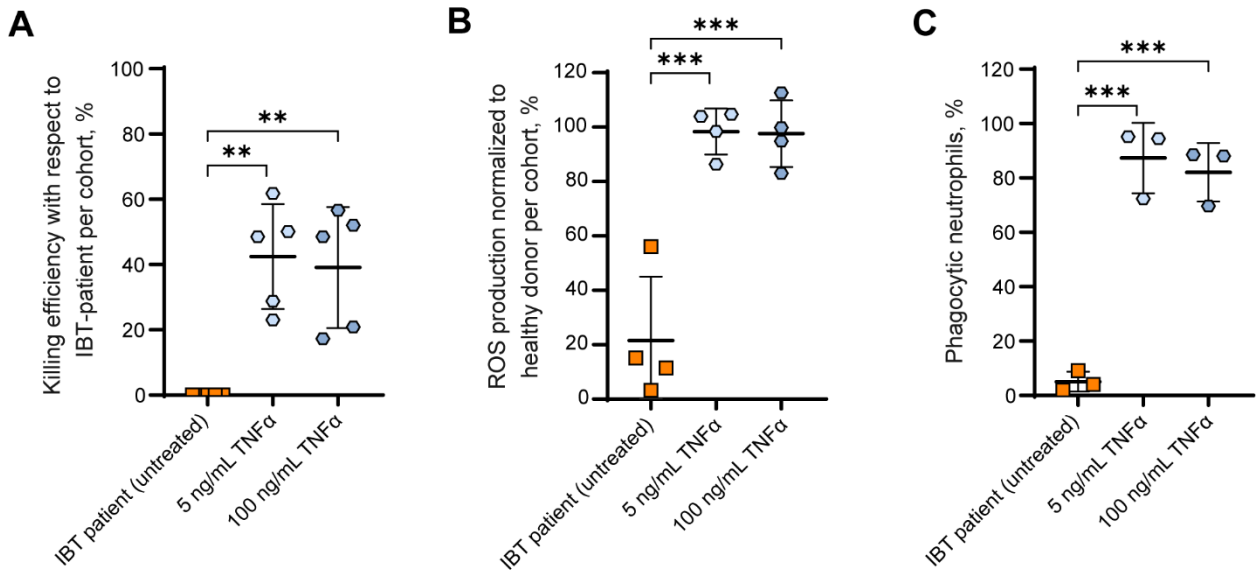

Figure 6. TNFα compensated for immune defects against *A. fumigatus* in neutrophils from IBT-treated patients. Human neutrophils from IBT-treated patients or healthy donors were incubated for 4h with TNFα and co-incubated with *A. fumigatus* B5233 strain for all figure panels. **(A)** Neutrophils were incubated with *A. fumigatus* (MOI:0.25) for 5h and metabolic activity was estimated by resazurin-based assay. Data are shown as the percentage of *A. fumigatus* killing efficiency corresponding to neutrophils from each IBT-treated patient. Error bars are SD, $n = 5$. **(B)** Neutrophils were incubated with 1 mg/mL *A. fumigatus* heat-killed hyphae. ROS production was measured by chemiluminescence using lucigenin. Data represents normalized ROS production from IBT-patient neutrophils to ROS production from healthy donors, per patient. Error bars are SD, $n = 4$. **(C)** Neutrophils were co-incubated with labeled *A. fumigatus* swollen spores (MOI: 10). The displayed percentage of phagocytic neutrophils (CD45-AF700$^+$/CD66b-APC$^+$/conidia-AF488$^+$) was estimated based on the total number of viable neutrophils (CD45-AF700$^+$/CD66b-APC$^+$). A minimum of 10,000 viable CD66b-APC$^+$ events were recorded. Data represents the percentage of phagocytic neutrophils for neutrophils from each IBT-treated patient. Because of limits placed on peripheral blood draws for these patients, not all assays were performed on the 5 patients. Error bars are SD, $n = 3$. ** $p < 0.01$; *** $p < 0.001$.

TABLES

TABLE 1

DEG from IBT-treated neutrophils vs DMSO-treated neutrophils (unstimulated).

Gene	Mean of log_2 fold-change (vs DMSO)	Std. error
ADGRG3	2.64	0.66
ALPL	2.84	0.558
APOL6	-1.58	0.324
CD274	-3.68	0.624
CR1	2.46	0.598
ERN1	1.65	0.209
FBXO6	-3.09	0.79
FOS	2.17	0.554
GBP1	-3.62	0.886
IL1RAP	2.17	0.547
IL1RL1	2.53	0.572
MAP2K4	1.54	0.218
PIK3CB	3.16	0.728
RAC2	1.5	0.322
STAT1	-1.96	0.186
TIMP2	1.53	0.198
TMEM140	1.83	0.436
TNF	-3.93	0.623